MRS Communications (2014), *4*, 159–170
© Materials Research Society, 2014
doi:10.1557/mrc.2014.34

MRS Communications

Prospective Articles

Understanding the relationship between $Cu_2ZnSn(S,Se)_4$ material properties and device performance

Talia Gershon, Tayfun Gokmen, Oki Gunawan, Richard Haight, and **Supratik Guha,** IBM TJ Watson Research Center, 1101 Kitchawan Road, Yorktown Heights, New York 10598
Byungha Shin, KAIST Department of Materials Science, Munji-ro 14, Yuseong-gu, Daejeon, South Korea
Address all correspondence to Talia Gershon at **tsgersho@us.ibm.com**

(Received 29 September 2014; accepted 12 November 2014)

Abstract

$Cu_2ZnSn(S,Se)_4$ (CZTSSe) photovoltaics (PV) have long been considered promising candidates for large-scale PV deployment due to the availability of constituent elements and steady improvements in device efficiency over time. The key limitation to high efficiency in this technology remains a deficit in the open-circuit voltage with respect to the band gap. The past decade has seen significant progress toward understanding how the various material properties such as bulk and surface composition, point defects (intrinsic and extrinsic), and grain boundaries all impact the optoelectronic properties of CZTSSe materials, and consequently device performance. This paper aims to summarize what is known about the CZTSSe bulk and surfaces, and how these material properties may be related to the Voc deficit.

Introduction

The kesterite compound $Cu_2ZnSn(S,Se)_4$ (CZTSSe) has attracted widespread interest for many years due to its optimal band gap (1.0–1.5 eV, depending on the chalcogen composition), the earth-abundance of its constituent elements, and the hope that it may one day replace $Cu(In,Ga)Se_2$ (CIGS) as a scalable commercial thin-film photovoltaic (PV) absorber material. Efficiencies have risen steadily to a certified champion value of 12.6% for the mixed sulfoselenide,[1] with demonstrated Jsc values reaching over 80% of the theoretical maximum. Meanwhile, the pure-selenide and pure-sulfide kesterites have reached record efficiencies of 11.6[2] and 9.2%,[3] respectively. However, the performance of CZTSSe devices still trails that of CIGS, largely due to a deficit in the open-circuit voltage (V_{oc}), which also limits the fill factor.[4] There have been numerous hypotheses for what is presently limiting the device V_{oc}. These can be grouped into three broad categories: a non-Ohmic back contact, a high degree of disorder and/or compensating defects in the CZTSSe bulk, and a poorly optimized interface with the buffer layer.

The current champion CZTSSe device architecture is largely borrowed from CIGS technology, where a soda-lime glass substrate, Mo bottom contact, CdS buffer layer, and ZnO/ITO bilayer electrode have been found to yield the highest performance.[1] The full device stack is thus: glass/Mo/CZTSSe/CdS/ZnO/ITO. We note that in high-efficiency CZTSSe devices, an interfacial $Mo(S,Se)_2$ layer is always present between the Mo and the CZTSSe. This interfacial layer is believed to be important for film adhesion and also for ensuring Ohmic contact with CIGS.[5,6] However, it may not be true that this contact is Ohmic for all CZTSSe materials. In some cases, when CZTSSe device efficiency is low, devices display low fill factor values and high series resistance. Using a recently developed technique involving monochromatic high-intensity Suns-V_{oc} measurements, it has been shown that a non-Ohmic barrier at the back contact opposing the main PV junction is present in these low FF devices, which also reduces the V_{oc} at 1 sun.[7] This Schottky behavior at the back contact is associated with a low-carrier density in the CZTSSe layer or possibly secondary phases at the back interface. However, this detrimental effect is negligible in high-efficiency CZTSSe devices,[7] where the back contact is found to be Ohmic.

Although alternative buffer layers have been explored,[8–10] a CdS buffer, prepared by chemical bath deposition, has still been found to produce the best device results. In studying the band alignment at the CZTSSe/CdS interface, a conduction band spike, or an energetic offset in which the conduction band of the CdS is positioned closer to the vacuum level than that in CZTSSe, has been found between the two materials with a height of ~0.41–0.48 eV.[11] A small conduction band spike can be beneficial to performance in that it helps suppress interfacial recombination; however, a large spike can be detrimental as it would create too large a barrier to electron flow from CZTSSe to the buffer; a 0.4 eV spike is believed to be acceptable for performance.[12] Alternative buffers such as In_2S_3 (also prepared by chemical bath deposition) have been identified as promising alternatives to CdS, with conduction band spikes of ~0.15 eV.[8] In contrast, ZnO is found to have a cliff-like band offset wherein the conduction band of ZnO is energetically positioned further from the vacuum level than that

https://doi.org/10.1557/mrc.2014.34 Published online by Cambridge University Press

in CZTSSe, leading to severe interfacial recombination and poor performance.[8] ZnS has too-large a conduction band spike, and carrier transport across the interface is inhibited.[8] Recent results suggest that a combined CdS/In_2S_3 buffer may offer yet further benefits for device performance.[13] The In_2S_3 component is believed to dope CZTSSe near the interface, improving the hole concentration and the quality of the junction and allowing the device characteristics such as the Suns-V_{oc} and temperature-dependent V_{oc} to more closely resemble those of CIGS. The efficiency of devices with this double-buffer was reported as 12.7% as measured internally, and 12.3% externally certified. It may be possible to achieve some further improvements by tuning the interface between CZTSSe and the buffer layer in this manner; however, to date the highest efficiencies are still achieved using a CdS-based buffer. The buffer layer, and the CZTSSe surface it mates with, will be discussed further at a later section of the manuscript.

This leaves us to focus predominantly on the CZTSSe bulk and interface and what is known regarding the relationship between CZTSSe material properties and device performance. Although the pentenary CZTSSe system is complex, there has been some progress toward understanding how the composition, phase diagram, microstructure, and point defect concentrations collectively interact to dictate the optoelectronic properties of CZTSSe thin films, single-crystal materials, internal surfaces, and ultimately device performance. Much of our current understanding of the material properties of CZTSSe stemmed from the early empirical observations that copper-poor, zinc-rich, and small-band gap (i.e., high selenium) compositions are optimal for performance.[4,14] Additionally, it has been known from an early stage that the presence of alkali species (e.g., Na and K) is beneficial to device operation. Building upon these empirical observations, extensive theoretical modeling and targeted experimental studies have further elucidated the reasons why device efficiencies improve under the above compositional conditions, which will be discussed throughout the present work.

This paper aims to summarize the current understanding of how various parameters, including bulk and surface compositions, point defects (intrinsic and extrinsic), and grain boundaries impact the optoelectronic properties of CZTSSe materials, as well as the performance of resulting devices. Ultimately, it is the hope that improved understanding will lead to enhanced device efficiencies in the future.

Metal ratios and bulk disorder

The highest-efficiency devices in the literature all have in common a zinc-rich and copper-poor (Cu/[Zn + Sn]) ~ 0.80–0.85, Zn/Sn ~1.1–1.2) thin-film stoichiometry.[15] There have been several hypotheses for why this off-stoichiometry is required for high efficiency. First, the phase diagrams of CZTS and CZTSe indicate a narrow region of phase stability, where slight excesses of Cu, Zn, or Sn result in the co-precipitation of CZTS(e) and its secondary phases such as Cu_2S(e), ZnS(e), $Cu_2SnS(e)_3$, and others.[14,16,17] Many of these phases, including Cu_2S(e), SnS(e), and $Cu_2SnS(e)_3$, are conductive and can shunt the device when present in the film.[16] Approaching zinc-rich and copper-poor compositions favors the precipitation of wider-E_g ZnS(e), which is not expected to trap electrons or holes, at the expense of the more conductive phases, thereby preventing a shunt mechanism. Surprisingly, CZTSe devices appear highly tolerant to the presence of secondary ZnS(e) phases; Vora et al. showed that increasing the Zn/Sn ratio from 1.15 to 2.1 only decreased the efficiency of CZTSe devices from 8.1 to 6.4%.[16]

First-principles calculations reveal a complicated composition-dependent point defect landscape in CZTS and CZTSe (Fig. 1). Significant disorder of Cu and Zn atoms on the Cu/Zn sublattice is expected for all compositions due to the chemical similarity of these atoms.[14,18] The Cu_{Zn} point defect would introduce an acceptor level, whereas the Zn_{Cu} defect would introduce a donor level; the [$Cu_{Zn} + Zn_{Cu}$] defect cluster is therefore a compensated defect pair. It is also found that the compensated defect pair [$V_{Cu} + Zn_{Cu}$] has relatively low formation energy and is therefore expected to form. Given that CZTS(e) is a *p*-type semiconductor, a net acceptor density is present amid the high degree of compensation, likely originating from a slight excess of either Cu_{Zn} or V_{Cu}. Experimental reports of the hole density in CZTS, CZTSe, and CZTSSe range from ~10^{15} to 10^{20} cm^{-3}, indicating a clear dependence of carrier concentration on sample preparation conditions and composition.[19–21]

Experimental studies of the CZTS atomic structure have indeed confirmed the presence of significant atomic disorder in the Cu/Zn sublattice.[22–24] Several studies have reported complete[22] or partial[24] disorder on the Cu/Zn sublattice by applying Rietveld analysis to neutron diffraction data. Another study directly observed regions of local Zn enrichment and Cu depletion via aberration-corrected scanning tunneling electron microscopy, with compositional fluctuations of the order of 1.5–5 nm reported.[23] Local Zn enrichment inherently implies a local segregation of donor defects, whereas local copper enrichment implies local segregation of acceptors. Thus, assuming these defects are ionized, the density of charged defects in the semiconductor fluctuates along with the compositional fluctuations. These charge fluctuations in turn cause electrostatic potential fluctuations of the conduction and valence bands, in a manner previously described by Shklovskii and Efros.[25] Thus, compositional fluctuations of this type can cause band tailing in CZTSSe.[26]

Low-temperature photoluminescence (PL) studies of CZTS materials and devices also support the presence of a large number of compensated donor–acceptor pairs in CZTS, of the order of 10^{19} cm^{-3},[26,27] which is high enough to form electrostatic potential fluctuations.[27,28] Higher concentrations of donor–acceptor pairs, as measureable in PL and other studies, are correlated with reductions in V_{oc} and fill factor values in devices.[29] Other room-temperature studies have detected the presence of significant band tailing in CZTSSe, likely

https://doi.org/10.1557/mrc.2014.34 Published online by Cambridge University Press

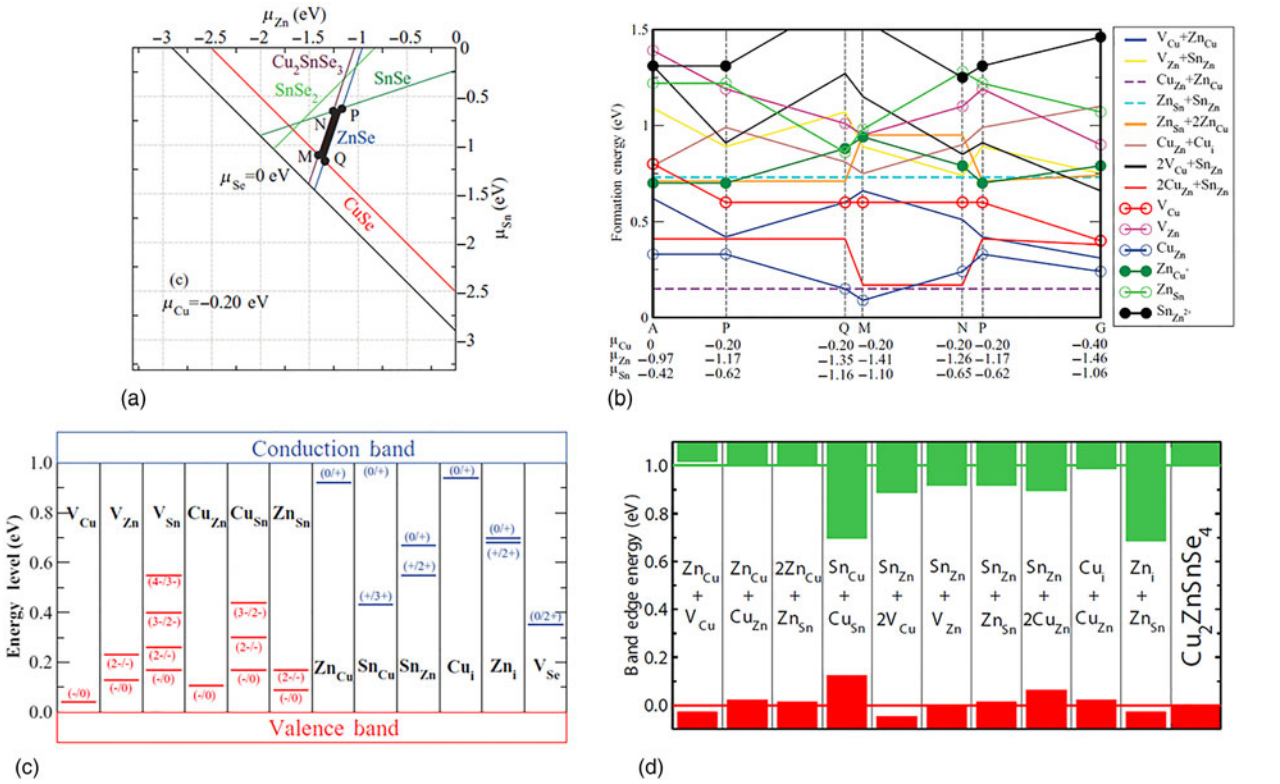


Figure 1. (a) The calculated stable region of the phase diagram for CZTSe as a function of zinc and tin chemical potentials (fixed copper chemical potential). (b) The calculated formation energies of various point defects and defect complexes in CZTSe as a function of chemical potential (specified in (a), *p*-type conditions were assumed). (c) The ionization energies of various point defects in the band gap of CZTSe, where red lines represent acceptors, blue lines represent donors, and the initial and final charge states are indicated in parentheses. (d) Calculated band gap shifts induced by various defect clusters in CZTSe, where red and green lines indicate the valence and conduction bands, respectively. Reproduced with permission.[14]

caused by disorder, which is again correlated with reductions in the V_{oc} values of CZTSSe devices.[26,30] These works examined both transient photocapacitance spectra[30] and sub-band gap absorption as measured via device EQE (Fig. 2)[26] and came to a similar conclusions that the presence of significant disorder in CZTSSe causes measureable band tailing, which in turn has a detrimental impact on V_{oc}. Recent work has even concluded that this band tailing may be severe enough to account for the entire observed V_{oc} deficit in CZTSSe.[31]

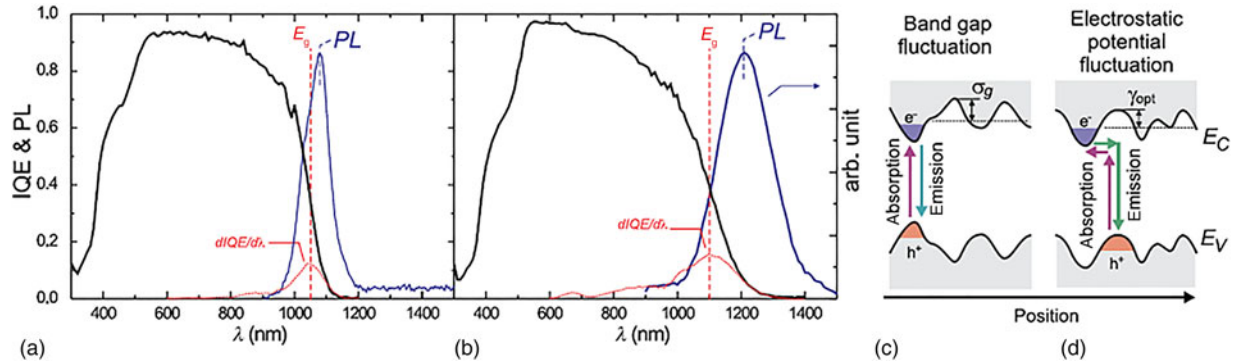


Figure 2. Internal quantum efficiency measurements overlaid with PL spectra from (a) high-efficiency CIGSSe (E_g = 1.19 eV) and (b) CZTSSe (E_g = 1.13 eV). (c) schematic of band gap fluctuations and electrostatic potential fluctuations, both of which could give rise to band tailing in the absorber. Reproduced with permission.[26]

https://doi.org/10.1557/mrc.2014.34 Published online by Cambridge University Press

The concentrations of various defect types appear to depend on sample stoichiometry. For example, Nagaoka et al. demonstrated control over the carrier concentration in single crystals of CZTS by changing the Cu:Zn ratio. A reduction of this ratio from 1.82 to 1.55 (i.e., a move toward copper-poor and zinc-rich conditions) led to a reduction in the carrier concentration by approximately one order of magnitude.[19] This appears to indicate a reduced acceptor density under copper-poor conditions. A similar finding has been observed in CZTSSe thin films.[21]

Furthermore, composition can also determine the likelihood of forming deep and detrimental defect clusters such as [Cu_{Zn} + Sn_{Zn}] and/or [$2Cu_{Zn}$ + Sn_{Zn}].[18] These are predicted to form more readily under zinc-poor conditions, which may help explain the better results obtained when the CZTSSe is prepared under zinc-rich conditions. Some studies also suggest that copper may preferentially occupy tin lattice sites as the copper content increases[32]; the Cu_{Sn} point defect is expected to contribute to a detrimental deep level in CZTSSe. Thus, the requirement for copper-poor and zinc-rich conditions to achieve high-efficiency CZTSSe devices appears related to the suppression of both undesirable secondary phases and harmful point defects and disorder in CZTS. We note that significant disorder has been observed in CZTSSe for nearly all compositions and preparations methods reported to date. As discussed above, it is likely that the main cause of this disorder is the compensating [Cu_{Zn} + Zn_{Cu}] defect cluster, which is predicted to have low formation energy independent of the composition.[14]

Sulfur and selenium

The sulfur-to-selenium ratio, or S/(S + Se), determines the band gap of CZTSSe, where the pure sulfide has a band gap of ~1.5 eV and the pure-selenide has a band gap of ~1.0 eV. The CZTSSe materials in the highest-efficiency devices reported to date have a selenium-rich composition and a band gap of ~1.13 eV.[1] This band gap is lower than the 1.34 eV band gap predicted by Shockley–Queisser considerations to produce the highest-efficiency devices under AM 1.5 G illumination.[33,34] However, the higher-sulfur CZTSSe compounds with more "optimal" band gaps typically display lower efficiencies and worse V_{oc} deficits. There are several likely explanations for the better performance observed from selenide materials.

First-principals calculations predict that both donor and acceptor defects are expected to produce shallower energy levels in the selenide materials, compared with the sulfides.[14,18] Experimental admittance spectroscopy studies have shown that indeed the depth of the acceptor level depends on the sulfur-to-selenium content, with shallower levels observed for selenide materials [Fig. 3(a)].[35] Another experimental study found that samples with higher sulfur content displayed not only deeper defects, but also an increase in bulk defect density, resulting in poorer carrier collection and higher rates of recombination.[36] Increasing sulfur content has been experimentally correlated with more severe band tailing in the absorbers and larger V_{oc} deficits in devices [Fig. 3(b)].[26] These phenomena are likely related in that deeper defects, and/or higher defect densities, are both expected to cause more severe band tailing and performance losses.

Sulfide compounds are also expected to exhibit larger electron effective masses and smaller dielectric constants than the selenides.[37] The reduction in dielectric constant with increasing sulfur has also been observed experimentally [Fig. 3(a)].[35] We note that a reduced dielectric constant would amplify all Coulombic (electrostatic) interactions because of reduced screening and hence may partially account for larger activation energies and more severe band tailing for sulfide compounds. The reduced screening of charged point defects in the material would also impact carrier mobility and recombination. This, coupled with a larger electron effective mass,[37] would result in poorer carrier transport through sulfide materials, as compared with selenides. A recent study examined minority carrier diffusion lengths (L_d) in CZTSSe materials with varying sulfur to selenium compositions and indeed found that this value decreased with increasing sulfur content (Fig. 4).[38]

Devices with high-sulfur CZTSSe have also been observed to have higher series resistance values than those with higher selenium content,[39–41] indicating that sulfur reduces bulk conductivity, mainly due to reduced carrier density[21] in the absorber, and makes the back contact less Ohmic. Note that even though a larger band gap tends to increase the V_{oc} and thus the FF (see, e.g., empirical relationship of V_{oc} and FF in Ref. 42) the monotonic increase in series resistance at higher band gap eventually degrades the FF, resulting in a maximum FF value when the CZTSSe band gaps is ~1.15 eV. This band-gap-dependent FF profile leads to the observed empirical optimum efficiency at ~1.15 eV.[1,43]

Finally, both sulfur and selenium are volatile at temperatures commonly used to prepare CZTSSe absorbers, with sulfur being the more volatile of the two chalcogen species. In many chalcogenide materials, chalcogen deficiency results in deep states, which are harmful to performance. Based simply on the higher vapor pressure of sulfur compared with selenium, one might expect that sulfur deficiency would be more difficult to avoid than selenium deficiency. Additionally, first-principles calculations suggest that sulfur vacancies have lower formation energies than selenium vacancies.[14] Thus, high-sulfur CZTSSe materials are expected to suffer more from the presence of deep recombination centers than are high-selenium materials.

Surface structure

Studies of the CZTSSe surface employing x-ray photoelectron spectroscopy (XPS) and other surface-sensitive techniques have found it to be highly depleted of copper, with respect to the bulk.[44,45] First-principles calculations find that charge-compensated point defects such as vacancies (V_{Cu}, V_{Zn}), antisites (Zn_{Cu}, Zn_{Sn}, Sn_{Zn}), and defect clusters (Cu_{Zn} + Cu_{Sn}, $2Zn_{Cu}$ + V_{Sn}) are required to stabilize the polar (112) surface, which is the preferred orientation of CZTSSe[46] (Fig. 5). In

https://doi.org/10.1557/mrc.2014.34 Published online by Cambridge University Press

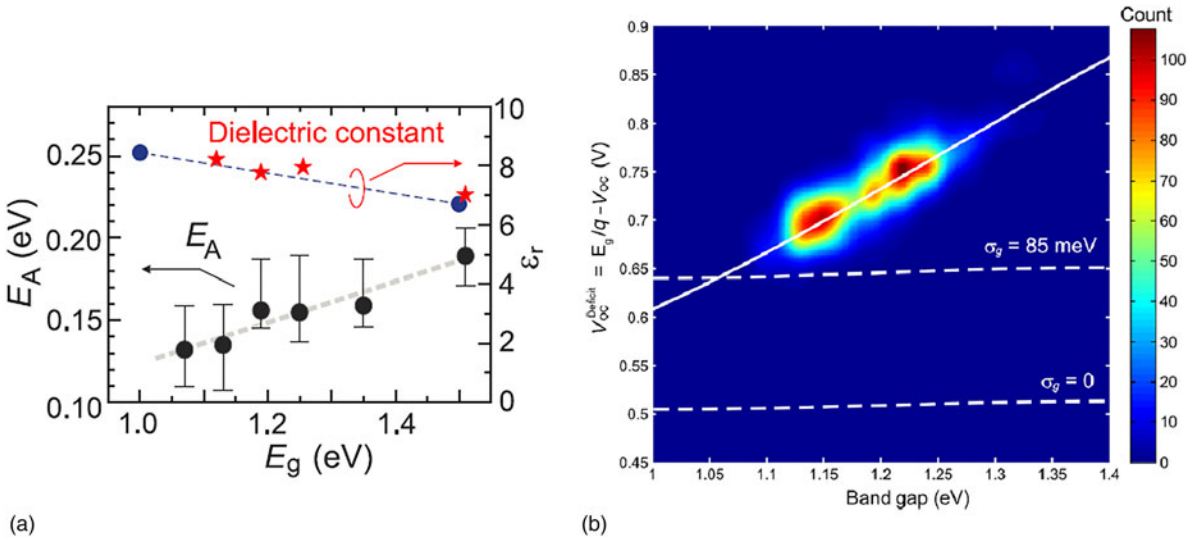


Figure 3. (a) Increase in activation energy of the acceptor level and simultaneous decrease in the dielectric constant in CZTSSe as the band gap of the absorber (i.e., sulfur content) increases. Reprinted with permission.[35] (b) Increase in the V_{oc} deficit as the band gap of the absorber (i.e., sulfur content) increases. Reproduced with permission.[26]

copper-poor, zinc-rich samples, the favored charge-stabilizing defects are those that are free from copper. The most prevalent point defects are predicted to be $2V_{Cu}$, $2Zn_{Cu} + 2V_{Sn}$ and Zn_{Sn}. These defects are also found not to contribute harmful states in the band gap. These calculations are consistent with what is experimentally observed of the CZTSSe surface, which indeed displays a copper-depleted character.

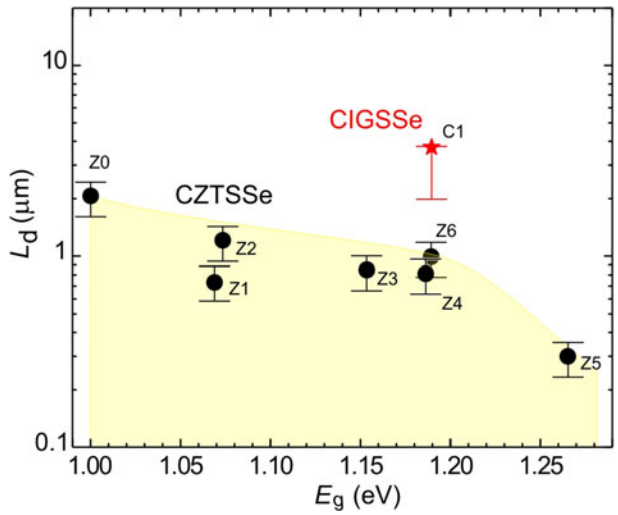


Figure 4. Minority carrier diffusion lengths in CZTSSe and CIGSSe materials of varying band gaps. The shaded region is a guide for the eye. Sample Z0 is a recent pure-selenide CZTSe sample, prepared by co-evaporation,[2] whereas the rest of the samples were reported in Ref. 38. Reprinted with permission.

Copper-depletion of the $CuInSe_2$ (CIS) surface has also been widely reported and studied.[47,48] In this system, it is also found that charged surface defects stabilize the (112) surface.[49] It has been reported that the so-called "ordered vacancy compound" (OVC) that spontaneously forms on the CIS surface has a much lower copper concentration ($CuIn_3Se_5$), is *n*-type, has a slightly larger band gap (1.3 eV, compared with 1.04 eV), and is responsible for forming a *p*–*n* junction with the CIS layer below.[48] Upon deposition of the buffer, the junction becomes CIS/OVC/CdS. Furthermore, Cd may diffuse into the OVC layer thereby further doping it *n*-type and improving the junction characteristics,[50] as cadmium is a known donor defect in CIS.[51]

An open question is: to what extent does the copper-deficient surface observed in CZTSSe resemble that observed in CIS and CIGS? If Cd inter-diffuses with the CZTSSe surface during chemical bath deposition, which sites does it occupy and what would the junction look like? One study examined these questions using first-principles analysis and found that substitution of cadmium onto Cu and Zn sites is more favorable than on Sn sites,[52] where Cd_{Cu} is a donor defect and Cd_{Zn} is neutral. More favorable still is the compensated defect complex ($Cd_{Cu} + V_{Cu}$). This defect pair is expected to dominate in equilibrium, with small amounts of Cd_{Cu} and Cd_{Zn} also present. If this were the case, the degree of *n*-type doping of the copper-poor CZTSSe surface would be limited compared with the CIS case; however, real experimental preparation conditions may not kinetically allow equilibrium to be reached. Non-equilibrium could therefore allow *n*-type doping of the surface region, in a manner similar to what is observed in CIS. These phenomena warrant further investigation to fully understand this interface and how it evolves during chemical bath deposition of the buffer.

https://doi.org/10.1557/mrc.2014.34 Published online by Cambridge University Press

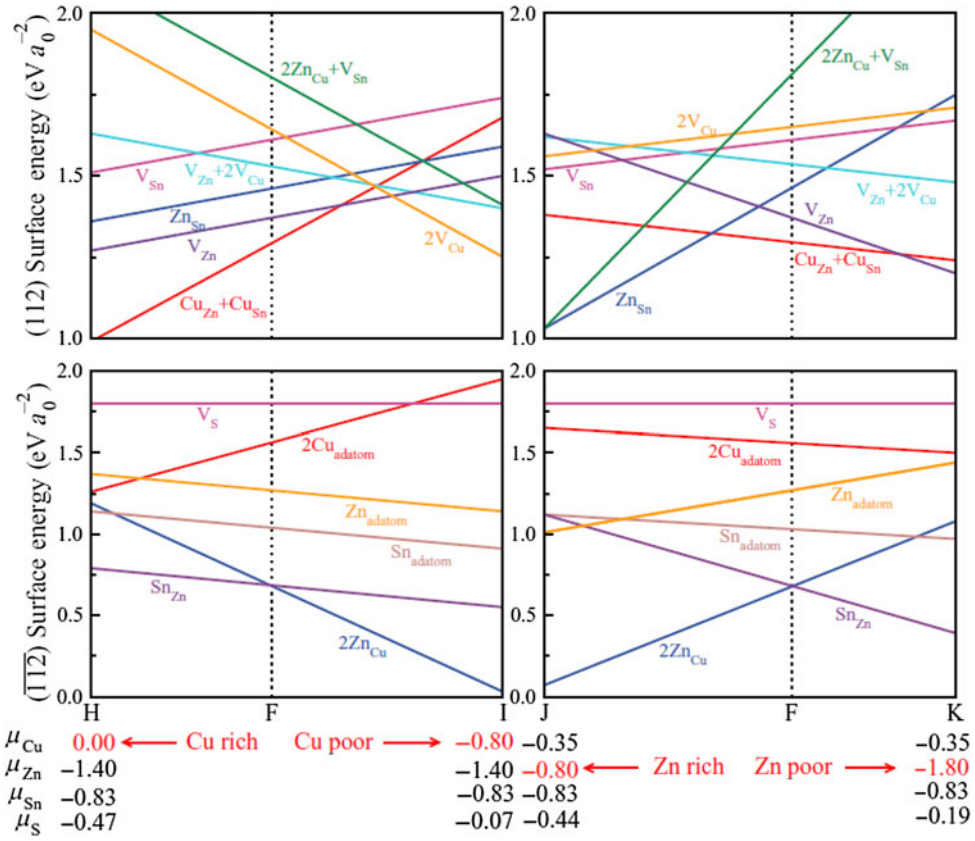


Figure 5. Defect formation energies on the (112) (top) and (112) (bottom) as a function of chemical potential (i.e., Cu rich, poor and Zn rich, poor). Reprinted with permission from Peng et al..[46] Copyright (2013) by the American Physical Society.

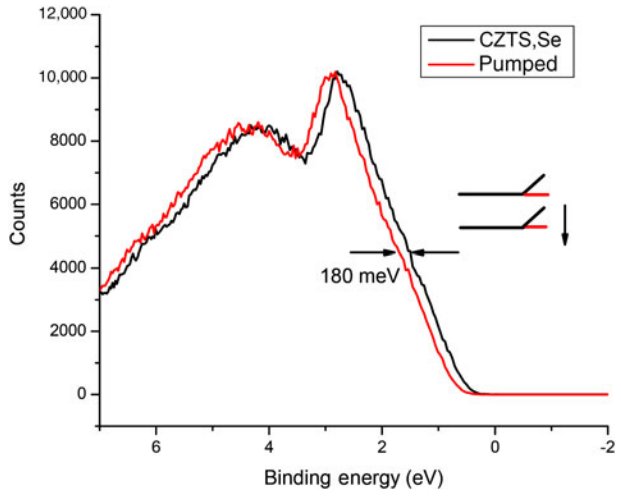


Figure 6. Femtosecond UPS spectra of air-annealed CZTSSe under equilibrium (unpumped, black) and flat band (pumped, red) conditions. The arrows indicate the shift of the spectrum following photoexcitation. The bands bend upwards, indicating a condition of accumulation at the surface. Reproduced with permission.[44]

Another notable aspect of the CZTSSe surface is that the CZTSSe bands are found to bend upwards, indicating a condition of accumulation.[44] Such upward band bending indicates that excess negative charge is trapped at or near the surface. This was determined using femtosecond pump (1.55 eV photon energy)/probe (26.35 eV) ultraviolet photoelectron spectroscopy (fs-UPS), where spectra are recorded both in equilibrium and flat-band (photoexcited) conditions and the spectra are compared with determine the direction of band bending (Fig. 6). Photoexcitation with an intense pulse of 800 nm light produces a dense electron–hole plasma that flattens the CZTSSe bands near the surface. Under photoexcitation, the bands shift to higher binding energy (red) indicating that under equilibrium the bands are bent up at the surface. An accumulated surface has been noted for CZTSSe samples with or without surface oxide layers removed, indicating a fundamental property of the CZTSSe surface. Haight et al. attribute the accumulation at the surface to the large copper deficiency in this region, where the copper vacancy is expected to act as a shallow acceptor in CZTSSe.

Air annealing of CZTSSe films prior to chemical bath deposition of CdS buffers has been shown to dramatically improve both absorber PL and device performance. Following air

https://doi.org/10.1557/mrc.2014.34 Published online by Cambridge University Press

anneal, strong sodium and oxygen signals are detected by XPS,[44] indicating both the formation of a surface oxide and diffusion of Na to the surface. Even following NH_4OH etching to remove oxygen and Na at the surface, secondary ion mass spectrometry (SIMS) reveals that the sodium and oxygen signals are present throughout the CZTSSe film thickness. However, the most likely location for most of the sodium and oxygen species detected is at grain surfaces rather than the grain interior.[53] The presence of sodium and oxygen at the grain surfaces in high-efficiency CIS, CIGS, and CZTSSe has been correlated with high device performance. One explanation for this observed relationship is that Na may aid in the oxidation of grain boundaries, i.e., the filling of chalcogen vacancies with oxygen, which could help passivate deep defects along these boundaries.[44,54] Similar observations on the efficacy of air anneals in CIS-based devices are consistent with our understanding of diffusion of O and Na along grain boundaries and their effect on grain boundary passivation.[44,55]

Alkali impurities

Much like in CIGS materials, sodium and other alkali species are found to be important for achieving high-efficiency CZTSSe devices. In particular, sodium is found to increase grain size,[56,57] increase carrier concentration and/or mobility,[58–62] passivate deep defects,[54,63,64] and improve the fill factors and open-circuit voltages of CZTSSe devices.[63,65,66] It has been found that potassium behaves in a manner similar to sodium in CZTS.[67]

Surface compositional studies of high-efficiency CZTSSe absorbers have found that sodium is present in large concentrations at surfaces and grain boundaries in CZTSSe.[44,53] First-principles studies suggest while grain boundaries in CIGS are fundamentally electrically benign,[68] unpassivated grain boundaries in CZTSe contribute deep states which are expected to act as non-radiative recombination centers.[69] Kelvin-probe studies have found potential "spikes" at grain boundaries in CZTSSe, which have been proposed to behave as hole-repelling and electron-attracting regions, aiding the separation and transport of the minority electrons.[70] However, these spikes may not exist in materials that do not contain sodium.[70] These results seem to suggest that sodium segregates to grain boundaries, and once there may be important for suppressing non-radiative recombination. This was further supported in a PL study, which examined the total PL intensity in CZTS as a function of sodium, and as a function of temperature.[64] It was found that at all temperatures, samples with less sodium luminesced less than those with more sodium. Furthermore, as the temperature increased from ~4 K toward room temperature, the PL of samples with little or no sodium dropped at a much higher rate than samples with more sodium, indicating that when carriers had enough thermal energy to travel longer distances, they tended to reach non-radiative recombination centers, likely along grain boundaries [Fig. 7(f)]. Once sufficient sodium was present in the films, samples with vastly different grain sizes (and thus boundary densities) displayed identical radiative recombination profiles, indicating that the grain boundaries had become passive within the detection limits of the study.[64]

In addition to passivating grain boundaries, alkali species significantly improve CZTSSe microstructure by enhancing grain size[56,57,64,67,71] [Figs. 7(a)–7(d)]. It is believed that this microstructural improvement is related to the formation of a liquid sodium–chalcogen-based phase at the grain boundaries. Enhanced diffusion through a phase such as this is especially important in zinc-rich and copper-poor materials, where ZnS(e) must be expelled from growing CZTSSe grains and may drag on advancing grain boundaries, prevent grain growth, if not removed from these boundaries.[64,71] It has been shown that the distribution of zinc throughout CZTS thin films is heavily influenced by the concentration of sodium present in the absorber during the annealing stage [Fig. 7(e)]. A large average grain size in CZTS was correlated with a reduction in zinc content through the film bulk and simultaneously the accumulation of zinc sulfide toward the back interface near the Mo contact. The phase diagram of the Zn–Na–S system indicates a eutectic temperature of roughly 610 °C.[72] This may help explain why annealing at such high temperatures is required to achieve large grains in CZTSSe.[73] Another study showed that even CZTS films prepared on alkali-free substrates could display these large grain size improvements when soda-lime glass substrates were placed in the same annealing ampoule, implying that alkali species may volatilize out of the glass during the anneal and impact the microstructure.[67]

Sodium may also incorporate directly onto the CZTS lattice. Studies on single-crystals have found an increase in the unit-cell size upon incorporation of sodium as measured by x-ray diffraction,[62] indicating the incorporation of sodium into the structure. This finding was also correlated with an increase in both the carrier concentration and mobility of CZTS. The authors attributed this to a reduction in the acceptor activation energy and a reduction in point defect compensation in the CZTS structure. Enhanced fill factors and V_{oc} values of CZTSe devices have been attributed to improvements in carrier concentration and mobility seen upon sodium incorporation into CZTSe.[65]

Other substitutional elements in CZTS

Although it is possible to change the band gap in CZTSSe by varying the sulfur to selenium content, it appears that sulfur may have other detrimental impacts on device performance (see above). Other chemical variations to CZTSSe can also induce band gap changes. First-principles calculations find that Ge and Si may be alloyed into the CZTSSe structure, substituting onto the tin site, to increase the band gap [Fig. 8(a)].[74] It was found that Ge is highly miscible into CZTSe with the $Cu_2Zn(Ge,Sn)Se_4$ band gap ranging from 1.0 eV for the pure-tin compound and 1.5 eV for the pure-Ge compound. Band gap tunability has been demonstrated experimentally in the $Cu_2Zn(Ge,Sn)S_4$ system, where Ford et al. prepared films with band gaps ranging from 1.5 eV (pure tin Cu_2ZnSnS_4) to

https://doi.org/10.1557/mrc.2014.34 Published online by Cambridge University Press

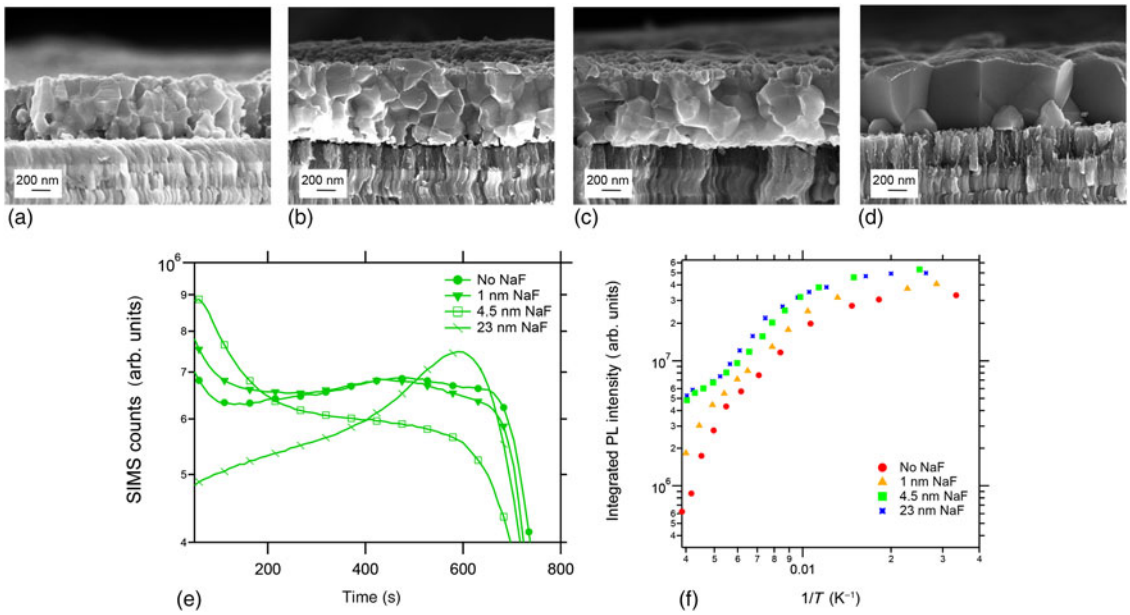


Figure 7. SEM cross-sectional images of CZTS thin films where (a) 0 nm, (b) 1 nm, (c) 4.5 nm, and (d) 23 nm of NaF was evaporated onto the substrate prior to CZTS growth and annealing. (e) SIMS depth profile of zinc distribution in the samples in (a-d). (f) Integrated PL intensity of the samples in (a–d) as a function of temperature. Reproduced with permission.[64]

1.94 eV (pure Ge Cu_2ZnGeS_4), with various values in between [Fig. 8(c)].[75] The magnitude of this shift is consistent with theoretical predictions.[74] The same group later demonstrated efficiencies as high as 8.4% (without anti-reflection coating) using a partially Ge substituted kesterite material.[76] In the same year, Bag et al. reported an efficiency of 9.1% by substituting 40% Ge into CZTSe.[77] This group demonstrated effective Ge incorporation by monitoring the x-ray diffraction peak, which shifts to larger 2-theta with increasing Ge due to the smaller atomic size of Ge as compared with Sn. Silicon is less miscible in CZTSe, but offers a larger range of band gap tuning up to 2.4 eV for the $Cu_2ZnSiSe_4$ compound. In both cases (substitutional Ge or Si), the band gap change is expected to stem largely from a conduction band shift [Fig. 8(b)].

Furthermore, it was recently found that compounds in the I_2–II–IV–VI_4 family are generally stable when I = Cu, Ag, II = Zn, Cd, Hg, IV = Si, Ge, Sn, and VI = S, Se, and/or Te. Instability arises when II = Mg, Ca, Sr, Ba, when IV = Ti, Zr, Hf, or when IV = O due to competition from the related binary and ternary compounds.[78] The authors noted that phase

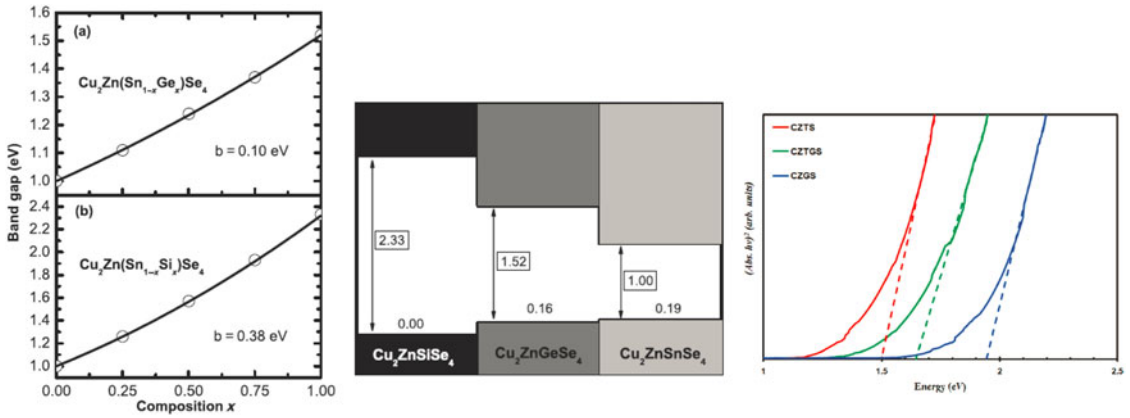


Figure 8. (a) Calculated dependence of the band gap of CZTSe as a function of Ge (top) and Si (bottom) substitution for Sn. (b) Predicted conduction and valence band positions of CZSiSe and CZGeSe, compared to CZTSe. (a) and (b) are reprinted with permission from Shu et al..[74] Copyright (2013) by the American Physical Society. (c) Experimental observation of band gap changes in CZTS as Ge is increasingly substituted for Sn. Reproduced with permission.[75]

https://doi.org/10.1557/mrc.2014.34 Published online by Cambridge University Press

separation is expected predominantly when the secondary phases had non-tetrahedral structures. This study opens up many possibilities to find a variant of CZTSSe that may have preferable optoelectronic properties and a lower propensity to self-compensate. Many of the possible substitutions mentioned above have never been reported experimentally, although they are promising materials to study in the future.

Prospectives

Over the past decade, our understanding of the factors impacting the material properties of CZTSSe, and consequently device performance, has improved dramatically. Through careful materials and device characterization, several key phenomena have been identified as likely culprits for the observed V_{oc} deficit in CZTSSe devices. Among these are the severity of the point defects and disorder within the CZTSSe bulk, which exceeds that observed in CIGS materials of the same band gap. It is believed that the higher degree of disorder is due to the chemical similarity of Cu and Zn atoms, and the low energetic barrier to the exchange of lattice positions amongst these two atoms. The disorder on the Cu/Zn sublattice may be responsible for the significant band tailing observed in the CZTSSe system, and therefore at least part of the V_{oc} deficit. It is possible that this disorder could be mitigated by an external stimulus, e.g., strain. Alternatively, recent theoretical calculations have indicated that the CZTSSe structure would be stable to various substitutions on the I, II, IV, and VI sites. By replacing either Cu, Zn, or both, a new I_2–II–IV–VI_4 compound may be identified

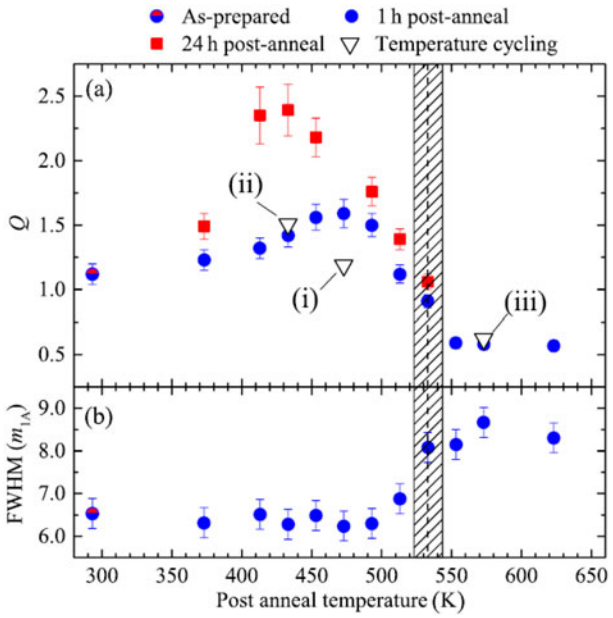


Figure 9. (top) Variation in "Q" (defined as an ordering parameter) for CZTS films annealed at different temperatures, for different durations. (bottom) Full-width at half maximum of the main Raman mode in CZTS samples annealed for 1 h at various temperatures. Shaded region indicates an "order/disorder" temperature. Reproduced with permission.[79]

that is less susceptible to the kind of disorder that causes detrimental band tailing and thus V_{oc} loss in the CZTSSe system.

Additionally, it has been proposed that disorder in CZTSSe may be reduced through low-temperature annealing for extended periods of time.[79] A recent study documented improvements in an "ordering parameter" of CZTS materials when samples were annealed below ~250 °C, as measured via Raman spectroscopy. It was found that these low-temperature anneals reduced the full-width at half-maximum of the main CZTS Raman peak centered at ~338 cm^{-1} (Fig. 9). The authors attributed the observed narrowing of the Raman peak to a reduction in the disorder of the bulk CZTS, i.e., fewer Cu–Zn antisites. The effect was found to be reversible, in that the Raman peak width of samples annealed above this temperature widened again, after initially decreasing during the low-temperature anneal. If it is indeed possible to reduce the disorder in CZTS using long low-temperature anneals without otherwise harming other material properties, this could offer a valuable means of reducing the V_{oc} deficit in CZTS devices. To date, there have been no published reports of device improvements using this technique.

We have also seen experimental and theoretical evidence that moving away from sulfur and toward a pure-selenide material improves the overall bulk properties of the absorber. This observation has recently manifested in a record V_{oc} deficit of 578 mV in a pure-selenide CZTSe device.[2] Although there seems to be a limit to the selenium content accessible via solution-processing due to solubility constraints, it is possible to prepare pure-selenide materials using vapor phase methods such as sputtering and co-evaporation. Unfortunately, the band gap of the pure CZTSe material (1.0 eV) is lower than the optimal value for high-efficiency single-absorber devices based on the Shockley–Queisser limit model.[33,34] If a method is found to increase the band gap of CZTSe without compromising its optoelectronic properties, we could see performance improvements above the 12.6% efficiency benchmark that has already been demonstrated. Alternatively, if methods are found to increase the dielectric constant of the absorber or reduce the electron effective mass, i.e., induce the opposite effect to what is observed with increasing sulfur, then device performance is also expected to increase.

Recent work has offered important insights into the chemical and electronic properties of the CZTSSe surface. Many similarities have been found between the CZTSSe surface and that of CIS; however, the interface chemistry that occurs during junction formation is still not fully understood. Additional work is needed to elucidate what if any losses in performance are caused by an unoptimized interface between CZTSSe and its buffer layer. It has been shown that formation of a double-emitter comprised CdS/In_2S_3 improves the junction characteristics such that CZTSSe devices behave more like CIGS devices, in terms of temperature-dependent V_{oc} and Suns-V_{oc}. This indicates that the CZTSSe/buffer interface may not yet be fully optimized and that further efficiency improvements may be possible as we learn more about the chemical and electrical

https://doi.org/10.1557/mrc.2014.34 Published online by Cambridge University Press

properties of the CZTSSe surface and the junctions it forms with buffer materials.

Some optimizations of the device layer thicknesses may also provide additional benefits. The CZTSSe layer in the highest-efficiency CZTSSe devices is typically 2–2.5 μm thick. This layer thickness is typically chosen because the hydrazine solution process used to prepare CZTSSe often results in voids toward the back of the absorber and thus multiple layers and a thick coating appear necessary to prevent detrimental device shunting through pinholes. Recent work has found that the minority carrier diffusion length in our high-efficiency CZTSSe layers ($E_g \sim 1.15$ eV) is closer to ~1.2 μm or less,[38] indicating that much of the CZTSSe thickness is inactive and/or possibly contributing to series resistance in the device. An optimized device might therefore employ films with thicknesses closer to the minority carrier diffusion length if methods can be found to suppress void formation toward the back contact and thereby avoid pinholes and shunt paths in the films.

Finally, high-efficiency CIGS devices typically contain a graded band gap structure, where the band gap increases slightly toward the front and back of the absorber layer to minimize recombination. Although this is generally acknowledged to be a promising route toward achieving improved device performance in CZTSSe,[4] no experimental studies demonstrating this effect have been reported. As discussed above, surface alloying with Ge, Si, and/or sulfur would allow a slight increase in the band gap at the CZTSSe surface.

Acknowledgments

The information, data, or work presented herein was funded in part by the U.S. Department of Energy, Energy Efficiency and Renewable Energy Program, under Award Number DE EE0006334. Neither the United States Government nor any agency thereof, nor any of their employees, makes any warranty, express or implied, or assumes any legal liability or responsibility for the accuracy, completeness, or usefulness of any information, apparatus, product, or process disclosed, or represents that its use would not infringe privately owned rights. Reference herein to any specific commercial product, process, or service by trade name, trademark, manufacturer, or otherwise does not necessarily constitute or imply its endorsement, recommendation, or favoring by the United States Government or any agency thereof. The views and opinions of authors expressed herein do not necessarily state or reflect those of the United States Government or any agency thereof.

References

1. W. Wang, M.T. Winkler, O. Gunawan, T. Gokmen, T.K. Todorov, Y. Zhu, and D.B. Mitzi: Device characteristics of CZTSSe thin-film solar cells with 12.6% efficiency. *Adv. Energy Mater.* **4**, (2014).
2. Y.S. Lee, T. Gershon, O. Gunawan, T.K. Todorov, B. Shin, Y. Virgus, and S. Guha: $Cu_2ZnSnSe_4$ thin-film solar cells by thermal co-evaporation with 11.6% power conversion efficiency and improved minority carrier diffusion length. *Adv. Energy Mater.* (2014), DOI: 10.1002/aenm.201401372.
3. T. Kato, H. Hiroi, N. Sakai, S. Muraoka, and H. Sugimoto: Characterization of front and back interfaces on Cu_2ZnSnS_4 thin-film solar cells. In *Proc. of the 27th EU-PVSEC.* Vol. 2236 (2012).
4. D.B. Mitzi, O. Gunawan, T.K. Todorov, and D.A.R. Barkhouse: Prospects and performance limitations for Cu–Zn–Sn–S–Se photovoltaic technology. *Philos. Trans. R. Soc. A* **371**, 20110432 (2013).
5. N. Kohara, S. Nishiwaki, Y. Hashimoto, T. Negami, and T. Wada: Electrical properties of the Cu(In,Ga)Se_2/$MoSe_2$/Mo structure. *Sol. Energy Mater. Sol. Cells* **67**, 209 (2001).
6. D. Abou-Ras, G. Kostorz, D. Bremaud, M. Kälin, F. Kurdesau, A. Tiwari, and M. Döbeli: Formation and characterisation of $MoSe_2$ for Cu(In,Ga)Se_2 based solar cells. *Thin Solid Films* **480**, 433 (2005).
7. O. Gunawan, T. Gokmen, and D.B. Mitzi: Suns-VOC characteristics of high performance kesterite solar cells. *J. Appl. Phys.* **116**, (2014).
8. D.A.R. Barkhouse, R. Haight, N. Sakai, H. Hiroi, H. Sugimoto, and D. B. Mitzi: Cd-free buffer layer materials on $Cu_2ZnSn(S_xSe_{1-x})4$: Band alignments with ZnO, ZnS, and In_2S_3. *Appl. Phys. Lett.* **100**, (2012).
9. H. Hiroi, N. Sakai, S. Muraoka, T. Katou, and H. Sugimoto: Development of high efficiency Cu_2ZnSnS_4 submodule with Cd-free buffer layer. In *Photovoltaic Specialists Conf. (PVSC), 2012 38th IEEE* (IEEE, 2012), p. 001811.
10. N. Sakai, H. Hiroi, and H. Sugimoto: Development of Cd-free buffer layer for Cu_2ZnSnS_4 thin-film solar cells. In *Photovoltaic Specialists Conf. (PVSC), 2011 37th IEEE* (IEEE, 2011), Seattle, WA, p. 003654.
11. R. Haight, A. Barkhouse, O. Gunawan, B. Shin, M. Copel, M. Hopstaken, and D.B. Mitzi: Band alignment at the $Cu_2ZnSn(S_xSe_{1-x})4$/CdS interface. *Appl. Phys. Lett.* **98**, (2011).
12. J. Nelson: *The Physics of Solar Cells* (Imperial College Press, London, 2003).
13. J. Kim, H. Hiroi, T.K. Todorov, O. Gunawan, M. Kuwahara, T. Gokmen, D. Nair, M. Hopstaken, B. Shin, Y.S. Lee, W. Wang, H. Sugimoto, and D.B. Mitzi: High efficiency $Cu_2ZnSn(S,Se)_4$ solar cells by applying a double In_2S_3/CdS emitter. *Adv. Mater.* (2014). DOI: 10.1002/adma.201402373.
14. S. Chen, A. Walsh, X.-G. Gong, and S.-H. Wei: Classification of lattice defects in the kesterite Cu_2ZnSnS_4 and $Cu_2ZnSnSe_4$ Earth-abundant solar cell absorbers. *Adv. Mater.* **25**, 1522 (2013).
15. H. Katagiri, K. Jimbo, M. Tahara, H. Araki, and K. Oishi: The influence of the composition ratio on CZTS-based thin film solar cells. In *MRS Proc.* (Cambridge University Press, vol. 1165, 2009), p. 1165
16. N. Vora, J. Blackburn, I. Repins, C. Beall, B. To, J. Pankow, G. Teeter, M. Young, and R. Noufi: Phase identification and control of thin films deposited by co-evaporation of elemental Cu, Zn, Sn, and Se. *J. Vac. Sci. Technol. A* **30**, (2012).
17. S. Chen, J.-H. Yang, X. Gong, A. Walsh, and S.-H. Wei: Intrinsic point defects and complexes in the quaternary kesterite semiconductor Cu_2ZnSnS_4. *Phys. Rev. B* **81**, 245204 (2010).
18. S. Chen, L.-W. Wang, A. Walsh, X. Gong, and S.-H. Wei: Abundance of $Cu_{Zn} + Sn_{Zn}$ and $2Cu_{Zn} + Sn_{Zn}$ defect clusters in kesterite solar cells. *Appl. Phys. Lett.* **101**, 223901 (2012).
19. A. Nagaoka, H. Miyake, T. Taniyama, K. Kakimoto, and K. Yoshino: Correlation between intrinsic defects and electrical properties in the high-quality Cu_2ZnSnS_4 single crystal. *Appl. Phys. Lett.* **103**, 112107 (2013).
20. D.B. Mitzi, O. Gunawan, T.K. Todorov, K. Wang, and S. Guha: The path towards a high-performance solution-processed kesterite solar cell. *Sol. Energy Mater. Sol. Cells* **95**, 1421 (2011).
21. O. Gunawan, Y. Virgus, and K.F. Tai: A parallel dipole line system. *Appl. Phys. Lett.* (2014, submitted).
22. S. Schorr, H.-J. Hoebler, and M. Tovar: A neutron diffraction study of the stannite-kesterite solid solution series. *Eur. J. Mineral.* **19**, 65 (2007).
23. B.G. Mendis, M.D. Shannon, M.C. Goodman, J.D. Major, R. Claridge, D. P. Halliday, and K. Durose: Direct observation of Cu, Zn cation disorder in Cu_2ZnSnS_4 solar cell absorber material using aberration corrected scanning transmission electron microscopy. *Prog. Photovolt.* **22**, 24 (2014).
24. S. Schorr and M. Tovar: *BENSC Experimental Report.* (2006).
25. B.I. Shklovskii and A.L. Efros: *Electronic Properties of Doped Semiconductors* (Springer-Verlag, Berlin Heidelberg, 1984).
26. T. Gokmen, O. Gunawan, T.K. Todorov, and D.B. Mitzi: Band tailing and efficiency limitation in kesterite solar cells. *Appl. Phys. Lett.* **103**, 103506 (2013).

https://doi.org/10.1557/mrc.2014.34 Published online by Cambridge University Press

27. T. Gershon, B. Shin, N. Bojarczuk, T. Gokmen, S. Lu, and S. Guha: Photoluminescence characterization of a high-efficiency Cu_2ZnSnS_4 device. *J. Appl. Phys.* **114**, 154905 (2013).
28. M.J. Romero, H. Du, G. Teeter, Y. Yan, and M.M. Al-Jassim: Comparative study of the luminescence and intrinsic point defects in the kesterite Cu_2ZnSnS_4 and chalcopyrite $Cu(In,Ga)Se_2$ thin films used in photovoltaic applications. *Phys. Rev. B* **84**, 165324 (2011).
29. T. Gershon, B. Shin, T. Gokmen, S. Lu, N. Bojarczuk, and S. Guha: Relationship between Cu_2ZnSnS_4 quasi donor–acceptor pair density and solar cell efficiency. *Appl. Phys. Lett.* **103**, 193903 (2013).
30. D.W. Miller, C.W. Warren, O. Gunawan, T. Gokmen, D.B. Mitzi, and J.D. Cohen: Electronically active defects in the $Cu_2ZnSn(Se,S)_4$ alloys as revealed by transient photocapacitance spectroscopy. *Appl. Phys. Lett.* **101**, 142106 (2012).
31. T. Gokmen, O. Gunawan, and D.B. Mitzi: Semi-empirical device model for $Cu_2ZnSn(S,Se)_4$ solar cells. *Appl. Phys. Lett.* **105**, 033903 (2014).
32. T. Washio, H. Nozaki, T. Fukano, T. Motohiro, K. Jimbo, and H. Katagiri: Analysis of lattice site occupancy in kesterite structure of Cu_2ZnSnS_4 films using synchrotron radiation x-ray diffraction. *J. Appl. Phys.* **110**, 074511 (2011).
33. W. Shockley and H.J. Queisser: Detailed balance limit of efficiency of p-n junction solar cells. *J. Appl. Phys.* **32**, 510 (1961).
34. U. Rau and J. Werner: Radiative efficiency limits of solar cells with lateral band-gap fluctuations. *Appl. Phys. Lett.* **84**, 3735 (2004).
35. O. Gunawan, T. Gokmen, C.W. Warren, J.D. Cohen, T.K. Todorov, D.A. R. Barkhouse, S. Bag, J. Tang, B. Shin, and D.B. Mitzi: Electronic properties of the $Cu_2ZnSn(Se,S)_4$ absorber layer in solar cells as revealed by admittance spectroscopy and related methods. *Appl. Phys. Lett.* **100**, 253905 (2012).
36. H.S. Duan, W. Yang, B. Bob, C.J. Hsu, B. Lei, and Y. Yang: The role of sulfur in solution-processed $Cu_2ZnSn(S,Se)_4$ and its effect on defect properties. *Adv. Funct. Mater.* **23**, 1466 (2013).
37. C. Persson: Electronic and optical properties of Cu_2ZnSnS_4 and $Cu_2ZnSnSe_4$. *J. Appl. Phys.* **107**, 053710 (2010).
38. T. Gokmen, O. Gunawan, and D.B. Mitzi: Minority carrier diffusion length extraction in $Cu_2ZnSn(Se,S)_4$ solar cells. *J. Appl. Phys.* **114**, 114511 (2013).
39. O. Gunawan, T. Gokmen, and D.B. Mitzi: *Copper Zinc Tin Sulphide-Based Thin Film Solar Cells* (John Wiley & Sons, Hoboken, NJ, 2015).
40. I. Repins, C. Beall, N. Vora, C. DeHart, D. Kuciauskas, P. Dippo, B. To, J. Mann, W.-C. Hsu, and A. Goodrich: Co-evaporated $Cu_2ZnSnSe_4$ films and devices. *Sol. Energy Mater. Sol. Cells* **101**, 154 (2012).
41. B. Shin, O. Gunawan, Y. Zhu, N.A. Bojarczuk, S.J. Chey, and S. Guha: Thin film solar cell with 8.4% power conversion efficiency using an earth-abundant Cu_2ZnSnS_4 absorber. *Prog. Photovolt.* **21**, 72 (2013).
42. M.A. Green: Accuracy of analytical expressions for solar cell fill factors. *Sol. Cells* **7**, 337 (1982).
43. T.K. Todorov, J. Tang, S. Bag, O. Gunawan, T. Gokmen, Y. Zhu, and D. B. Mitzi: Beyond 11% efficiency: characteristics of state-of-the-art $Cu_2ZnSn(S,Se)_4$ solar cells. *Adv. Energy Mater.* **3**, 34 (2013).
44. R. Haight, X. Shao, W. Wang, and D.B. Mitzi: Electronic and elemental properties of the $Cu_2ZnSn(S,Se)_4$ surface and grain boundaries. *Appl. Phys. Lett.* **104**, (2014).
45. M. Bär, B.-A. Schubert, B. Marsen, S. Krause, S. Pookpanratana, T. Unold, L. Weinhardt, C. Heske, and H.-W. Schock: Native oxidation and Cu-poor surface structure of thin film Cu_2ZnSnS_4 solar cell absorbers. *Appl. Phys. Lett.* **99**, (2011).
46. P. Xu, S. Chen, B. Huang, H.-J. Xiang, X.-G. Gong, and S.-H. Wei: Stability and electronic structure of Cu_2ZnSnS_4 surfaces: first-principles study. *Phys. Rev. B* **88**, 045427 (2013).
47. D. Liao and A. Rockett: Cu depletion at the $CuInSe_2$ surface. *Appl. Phys. Lett.* **82**, 2829 (2003).
48. D. Schmid, M. Ruckh, F. Grunwald, and H.-W. Schock: Chalcopyrite/defect chalcopyrite heterojunctions on the basis of $CuInSe_2$. *J. Appl. Phys.* **73**, 2902 (1993).
49. J.E. Jaffe and A. Zunger: Defect-induced nonpolar-to-polar transition at the surface of chalcopyrite semiconductors. *Phys. Rev. B* **64**, 241304 (2001).
50. D. Liao and A. Rockett: Cd doping at the $CuInSe_2$/CdS heterojunction. *J. Appl. Phys.* **93**, 9380 (2003).
51. P. Migliorato, J. Shay, H. Kasper, and S. Wagner: Analysis of the electrical and luminescent properties of $CuInSe_2$. *J. Appl. Phys.* **46**, 1777 (1975).
52. T. Maeda, S. Nakamura, and T. Wada: First-principles study on Cd doping in Cu_2ZnSnS_4 and $Cu_2ZnSnSe_4$. *Jpn. J. Appl. Phys.* **51**, 10NC11 (2012).
53. D.W. Niles, M. Al-Jassim, and K. Ramanathan: Direct observation of Na and O impurities at grain surfaces of $CuInSe_2$ thin films. *J. Vac. Sci. Technol A* **17**, 291 (1999).
54. L. Kronik, D. Cahen, and H.W. Schock: Effects of sodium on polycrystalline $Cu(In,Ga)Se_2$ and its solar cell performance. *Adv. Mater.* **10**, 31 (1998).
55. D. Cahen and R. Noufi: Defect chemical explanation for the effect of air anneal on CdS/$CuInSe_2$ solar cell performance. *Appl. Phys. Lett.* **54**, 558 (1989).
56. A. Rockett: The effect of Na in polycrystalline and epitaxial single-crystal $CuIn_{1-x}Ga_xSe_2$. *Thin Solid Films* **480**, 2 (2005).
57. W.H. Oo, J. Johnson, A. Bhatia, E. Lund, M. Nowell, and M. Scarpulla: Grain size and texture of Cu_2ZnSnS_4 thin films synthesized by cosputtering binary sulfides and annealing: effects of processing conditions and sodium. *J. Electron. Mater.* **40**, 2214 (2011).
58. T. Prabhakar and N. Jampana: Effect of sodium diffusion on the structural and electrical properties of Cu_2ZnSnS_4 thin films. *Sol. Energy Mater. Sol. Cells* **95**, 1001 (2011).
59. T. Nakada: Invited paper: CIGS-based thin film solar cells and modules: unique material properties. *Electon. Mater. Lett.* **8**, 179 (2012).
60. U. Rau and H.W. Schock: Electronic properties of $Cu(In,Ga)Se_2$ heterojunction solar cells–recent achievements, current understanding, and future challenges. *Appl. Phys. A* **69**, 131 (1999).
61. H. Zhou, T.-B. Song, W.-C. Hsu, S. Luo, S. Ye, H.-S. Duan, C.-J. Hsu, W. Yang, and Y. Yang: Rational defect passivation of $Cu_2ZnSn(S,Se)_4$ photovoltaics with solution-processed Cu_2ZnSnS_4: Na nanocrystals. *J. Am. Chem. Soc.* **135**, 15998 (2013).
62. A. Nagaoka, H. Miyake, T. Taniyama, K. Kakimoto, Y. Nose, M. A. Scarpulla, and K. Yoshino: Effects of sodium on electrical properties in Cu_2ZnSnS_4 single crystal. *Appl. Phys. Lett.* **104**, 152101 (2014).
63. P.T. Erslev, J.W. Lee, W.N. Shafarman, and J.D. Cohen: The influence of Na on metastable defect kinetics in CIGS materials. *Thin Solid Films* **517**, 2277 (2009).
64. T. Gershon, B. Shin, N. Bojarczuk, M. Hopstaken, D.B. Mitzi, and S. Guha: The role of sodium as a surfactant and suppressor of non-radiative recombination at internal surfaces in Cu_2ZnSnS_4. *Adv. Energy Mater.* (2014). DOI: 10.1002/aenm.201400849.
65. J.V. Li, D. Kuciauskas, M.R. Young, and I.L. Repins: Effects of sodium incorporation in Co-evaporated $Cu_2ZnSnSe_4$ thin-film solar cells. *Appl. Phys. Lett.* **102**, 163905 (2013).
66. T. Nakada, D. Iga, H. Ohbo, and A. Kunioka: Effects of sodium on $Cu(In,Ga)Se_2$-based thin films and solar cells. *Jpn. J. Appl. Phys.* **36**, 732 (1997).
67. M. Johnson, S. Baryshev, E. Thimsen, M. Manno, X. Zhang, I. Veryovkin, C. Leighton, and E. Aydil: Alkali-metal-enhanced grain growth in Cu_2ZnSnS_4 thin films. *Energy Environ. Sci.* **7**, 1931 (2014).
68. Y. Yan, C.-S. Jiang, R. Noufi, S.-H. Wei, H. Moutinho, and M. Al-Jassim: Electrically benign behavior of grain boundaries in polycrystalline $CuInSe_2$ films. *Phys. Rev. Lett.* **99**, 235504 (2007).
69. J. Li, D.B. Mitzi, and V.B. Shenoy: Structure and electronic properties of grain boundaries in earth-abundant photovoltaic absorber $Cu_2ZnSnSe_4$. *ACS Nano* **5**, 8613 (2011).
70. J.B. Li, V. Chawla, and B.M. Clemens: Investigating the role of grain boundaries in CZTS and CZTSSe thin film solar cells with scanning probe microscopy. *Adv. Mater.* **24**, 720 (2012).
71. C.M. Sutter-Fella, J.A. Stu"ckelberger, H. Hagendorfer, F. La Mattina, L. Kranz, S. Nishiwaki, A.R. Uhl, Y.E. Romanyuk, and A.N. Tiwari: Sodium assisted sintering of chalcogenides and its application to solution processed $Cu_2ZnSn(S,Se)_4$ thin film solar cells. *Chem. Mater.* **26**, 1420 (2014).
72. V. Tomashyk, P. Feychuk, and L. Shcherbak: *Ternary Alloys Based on II-VI Semiconductor Compounds* (Taylor & Frances Group, Boca Raton, FL, 2014).

https://doi.org/10.1557/mrc.2014.34 Published online by Cambridge University Press

73. B. Shin, Y. Zhu, N.A. Bojarczuk, S.J. Chey, and S. Guha: Control of an interfacial $MoSe_2$ layer in $Cu_2ZnSnSe_4$ thin film solar cells: 8.9% power conversion efficiency with a TiN diffusion barrier. *Appl. Phys. Lett.* **101**, 053903 (2012).
74. Q. Shu, J.-H. Yang, S. Chen, B. Huang, H. Xiang, X.-G. Gong, and S.-H. Wei: $Cu_2Zn(Sn,Ge)Se_4$ and $Cu_2Zn(Sn,Si)Se_4$ alloys as photovoltaic materials: structural and electronic properties. *Phys. Rev. B* **87**, 115208 (2013).
75. G.M. Ford, Q. Guo, R. Agrawal, and H.W. Hillhouse: Earth abundant element $Cu_2Zn(Sn_{1-x}Ge_x)S_4$ nanocrystals for tunable band gap solar cells: 6.8% efficient device fabrication. *Chem. Mater.* **23**, 2626 (2011).
76. Q. Guo, G.M. Ford, W.-C. Yang, C.J. Hages, H.W. Hillhouse, and R. Agrawal: Enhancing the performance of CZTSSe solar cells with Ge alloying. *Sol. Energy Mater. Sol. Cells* **105**, 132 (2012).
77. S. Bag, O. Gunawan, T. Gokmen, Y. Zhu, and D.B. Mitzi: Hydrazine-processed Ge-substituted CZTSe solar cells. *Chem. Mater.* **24**, 4588 (2012).
78. C. Wang, S. Chen, J.-H. Yang, L. Lang, H. Xiang, X. Gong, A. Walsh, and S.-H. Wei: Design of I2-II-IV-VI4 semiconductors through element-substitution: the thermodynamic stability limit and chemical trend. *Chem. Mater.* **26**, 3411 (2014).
79. J.J. Scragg, L. Choubrac, A. Lafond, T. Ericson, and C. Platzer-Björkman: A low-temperature order-disorder transition in Cu_2ZnSnS_4 thin films. *Appl. Phys. Lett.* **104**, 041911 (2014).

https://doi.org/10.1557/mrc.2014.34 Published online by Cambridge University Press